Annals of Hematology (2019) 98:2063–2072
https://doi.org/10.1007/s00277-019-03756-1

ORIGINAL ARTICLE

Effects of rigosertib on the osteo-hematopoietic niche in myelodysplastic syndromes

Ekaterina Balaian[1] · Heike Weidner[2,3] · Manja Wobus[1] · Ulrike Baschant[2,3] · Angela Jacobi[4] · Anna Mies[1] · Martin Bornhäuser[1,5,6] · Jochen Guck[4] · Lorenz C. Hofbauer[2,3,5] · Martina Rauner[2,3] · Uwe Platzbecker[7,8,9]

Received: 12 February 2019 / Accepted: 8 July 2019 / Published online: 16 July 2019

Abstract

Rigosertib is a novel multi-kinase inhibitor, which has clinical activity towards leukemic progenitor cells of patients with high-risk myelodysplastic syndromes (MDS) after failure or progression on hypomethylating agents. Since the bone marrow micro-environment plays an important role in MDS pathogenesis, we investigated the impact of rigosertib on cellular compartments within the osteo-hematopoietic niche. Healthy C57BL/6J mice treated with rigosertib for 3 weeks showed a mild suppression of hematopoiesis (hemoglobin and red blood cells, both − 16%, $p < 0.01$; white blood cells, − 34%, $p < 0.05$; platelets, − 38%, $p < 0.05$), whereas there was no difference in the number of hematopoietic stem cells in the bone marrow. Trabecular bone mass of the spine was reduced by rigosertib (− 16%, $p = 0.05$). This was accompanied by a lower trabecular number and thickness (− 6% and − 10%, respectively, $p < 0.05$), partly explained by the increase in osteoclast number and surface ($p < 0.01$). Milder effects of rigosertib on bone mass were detected in an MDS mouse model system (NHD13). However, rigosertib did not further aggravate MDS-associated cytopenia in NHD13 mice. Finally, we tested the effects of rigosertib on human mesenchymal stromal cells (MSC) in vitro and demonstrated reduced cell viability at nanomolar concentrations. Deterioration of the hematopoietic supportive capacity of MDS-MSC after rigosertib pretreatment demonstrated by decreased number of colony-forming units, especially in the monocytic lineage, further supports the idea of disturbed crosstalk within the osteo-hematopoietic niche mediated by rigosertib. Thus, rigosertib exerts inhibitory effects on the stromal components of the osteo-hematopoietic niche which may explain the dissociation between anti-leukemic activity and the absence of hematological improvement.

Keywords Rigosertib · Myelodysplastic syndromes · Osteoblasts · Mesenchymal stromal cells · Osteo-hematopoietic niche

Ekaterina Balaian and Heike Weidner contributed equally to this work.

Martina Rauner and Uwe Platzbecker contributed equally to this work.

Electronic supplementary material The online version of this article (https://doi.org/10.1007/s00277-019-03756-1) contains supplementary material, which is available to authorized users.

✉ Uwe Platzbecker
Uwe.Platzbecker@medizin.uni-leipzig.de

[1] Medical Clinic I, University Hospital Carl Gustav Carus Dresden, Dresden, Germany

[2] Medical Clinic III, University Hospital Carl Gustav Carus Dresden, Dresden, Germany

[3] Center for Healthy Aging, University Hospital Carl Gustav Carus Dresden, Dresden, Germany

[4] Biotechnology Center, Center for Molecular and Cellular Bioengineering, TU Dresden, Dresden, Germany

[5] German Cancer Consortium (DKTK), Partner Site Dresden and German Cancer Research Center (DKFZ), Heidelberg, Germany

[6] National Center for Tumor Diseases (NCT Partner Site Dresden), DKFZ, Heidelberg, Germany

[7] Medical Clinic and Policlinic 1, Hematology and Cellular Therapy, Leipzig University Hospital, Liebigstraße 22, 04103 Leipzig, Germany

[8] German MDS Study Group (G-MDS), Leipzig, Germany

[9] European Myelodysplastic Syndromes Cooperative Group (EMSCO group), http://www.emsco.eu

Introduction

Rigosertib is a novel drug with anticancer activity exerting its effects through a variety of mechanisms of action including indirect RAS-mimicry [1, 2], modulation of the PI3K-Akt-mTOR pathway, and disruption of mitosis through modulation of the polo-like kinase pathway [3, 4]. Recent chemical-genetic screening further revealed the destabilizing of microtubules as the main or possibly even singular mechanism of action [5]. Preclinical work demonstrating cytotoxic activity against leukemic cell lines [6, 7], in ex vivo and in vitro samples from patients with myelodysplastic syndromes (MDS) [8, 9], led to the development of several clinical trials in acute myeloid leukemia (AML) and MDS. These studies have demonstrated promising results, as well as good tolerability in certain subgroups of patients with high-risk MDS and AML, including those who have failed to respond to hypomethylating agent–based therapy [10–14].

The influence of rigosertib on the hematopoietic stem and progenitor cells (HSPC)/leukemic microenvironment is not yet fully described. There is only one publication demonstrating the role of this drug in the interaction between chronic lymphocytic leukemia (CLL) and stromal cells in lymph nodes [15]. Rigosertib abrogated the prosurvival effect of stromal cells on leukemic cells, however, did not directly affect stromal follicular dendritic cells. Importantly, rigosertib also potently blocked the migration of CLL cells towards SDF-1α, representing a chemokine secreted by different types of stroma cells that may guide migration of leukemic cells to the stromal microenvironment.

Given the prominent role of the osteo-hematopoietic niche in the pathogenesis of MDS [16, 17] and the lack of knowledge about the influence of rigosertib on the niche, the evaluation of possible mechanisms of action of this drug within the hematopoietic micromilieu may improve therapeutic treatment options.

Therefore, the aim of this study was to investigate the impact of rigosertib on the function of the osteo-hematopoietic niche.

Materials and methods

Studies in mice

All animal procedures were approved by the institutional animal care committee and the Federal state of Saxony. Mice were fed a standard diet as well as water ad libitum and were exposed to a 12-h light/dark cycle in an air-conditioned room at 23 °C. To assess the effects of rigosertib on healthy mice, 10-week-old male C57BL/6J wild-type (WT) mice were treated with rigosertib (250 mg/kg 3×/week i.p. for 3 weeks) or vehicle. The applied dosage corresponds to average one used in clinical trials. The same treatment conditions were used for 5-month-old NUP98-HOXD13 (NHD13) mice and their littermate WT mice. These mice express the *NUP98-HOXD13* fusion gene under the control of *vav1* regulatory elements leading to a transgenic expression of *NUP98-HOXD13* in hematopoietic cells and the development of cytopenia and blast excess due to MDS at the age of 4–6 months. Complete blood counts were done using Sysmex Blood Analyzer according to manufacturer's protocol. The femora and vertebrae were fixated in 4% PBS-buffered paraformaldehyde for 48 h and afterward analyzed to study bone microarchitecture after rigosertib treatment using micro-computed tomography (μCT, Scanco Medical, Switzerland) at a resolution of 10.5 μm. To investigate the osteoclast number as well as the osteoclast surface, the second and third vertebral bodies were embedded in paraffin. Bone slices (2 μm) were stained with tartrate-resistant acid phosphatase (TRAP). Histomorphometric osteoclast parameter was determined with the Osteomeasure software (OsteoMetrics, Atlanta, GA, USA).

ELISA

Procollagen type 1 N-terminal peptide (P1NP), a serum marker of bone formation, the bone resorption marker C-terminal collagen type I (CTX-1), and sclerostin as well as dickkopf 1 (Dkk-1) were measured in the serum using commercially available ELISAs.

Primary murine bone marrow stromal cell culture

Primary murine mesenchymal stromal cells (MSC) were yielded by flushing the femora with medium and maintaining plastic adherent cells in DMEM (Invitrogen) with 10% FCS and 1% penicillin/streptomycin. Cell viability was tested by Cell Titer Blue Assay (Promega, Mannheim, Germany). For this purpose, cells were seeded on the 96-well plate and cultured for 7 days in presence of 0.1 μM rigosertib or vehicle. After that, Cell Titer Blue Reagent was added for 1 h at 37 °C and the supernatant was assessed by fluorescence at 560/590 nm using the FluoStar Omega (BMG Labtech, Jena, Germany). Apoptosis was tested by Caspase-Glo 3/7 Assay. The reagent was added to each sample according to the manufacturer's protocol and incubated for 1 h using plate-shaker. The luminescence was measured in luminometer plates. For the assessment of osteoblastic differentiation, we used alizarin red staining and detection of ALP activity. Osteoblast cultures were fixed in 10% paraformaldehyde for 30 min and stained with 1% alizarin red S solution (pH 5.5, Sigma-Aldrich) for 10 min at room temperature. Excess dye was removed by repeatedly washing the plates with distilled water. The amount of incorporated calcium was eluted with 100 mM cetylpyridinium chloride (Sigma-Aldrich) for 10 min at room temperature. Aliquots were taken and measured photometrically at 540 nm in duplicates. ALP activity assay was

performed as follows: cells were lysed in 100 μl lysis buffer (1.5 mM Tris-HCl pH 7, 1 mM $ZnCl_2$, 1 mM $MgCl_2$, 1% triton X-100) and centrifuged for 20 min at 6,000 rpm at 4 °C. Aliquots of each sample were incubated with 100 μl alkaline phosphatase (ALP) substrate buffer (100 mM diethanolamine, 0.1% triton X-100 supplemented with 1:10 37 mM p-nitrophenyl phosphate) for 30 min at 37 °C. The enzymatic reaction was stopped with 40 mM NaOH, measured at a wavelength of 405 nm, and normalized to the total protein content determined by the BCA method from the same protein extracts.

Flow cytometry

The murine bone marrow cells were flushed from the femora with PBS and washed with PBS with 2% FCS. Thereafter, cells were stained with anti-murine antibodies for 30 min at 4 °C. Following washing steps with PBS/FCS (2%), cells were analyzed using the BD LSR II. For analysis of the gained data, FlowJo Version 10 was used. For the measurement of LSK cells, the following antibodies were used: APC Cy7-labeled c-kit, PECy5-labeled Sca-1, and FITC-labeled CD3, CD19, NK1.1, Ter119, CD11b, and CD45R as well as Gr1. LSK phenotype was defined as Lin^- c-kit^+ Sca-1^+. To characterize the erythroid populations, the following antibodies were used: PECy7-labeled CD45, PE-labeled CD71, and FITC-labeled Ter119. Cells with phenotype $CD45^-$ $CD71^+$ $Ter119^{low}$ were recognized as early erythroblasts (E1), whereas $Ter119^{high}$ as late erythroblasts.

Culture of primary human mesenchymal stromal cells

All procedures followed were in accordance with the ethical standards of the responsible committee on human experimentation and with the Helsinki Declaration of 1975, as revised in 2008. Informed consent was obtained from all patients for being included in the study. Primary human mesenchymal stromal cells (MSC) were collected from healthy young donors (aged 22–49 years, both genders), elderly donors (55–89 years, both genders), and MDS patients (45–78 years, both genders), and cultured according to modifications of previously reported methods [18]. Cells were maintained in DMEM (Invitrogen) with 10% FCS (Invitrogen) and 1% penicillin/streptomycin (PAA) and were used in passages 1–5. The cells have been routinely tested by flow cytometry for CD73, CD90, CD105, CD146, CD166, and CD44 surface markers and for their osteogenic and adipogenic differentiation potential. To generate osteogenic cells, 70% confluent cells were switched to basal medium supplemented with 100 μM ascorbate phosphate, 5 mM β-glycerol phosphate, and 10 nM dexamethasone (all from Sigma-Aldrich) for 7–10 days. Cells were treated with rigosertib (0.05–5 μM, Onconova) every each day. Rigosertib was diluted in dimethyl sulfoxide at the stock concentration of 50 μM and stored at − 80 °C protected from the direct light at all steps. Cell viability was tested by Cell Titer Blue Assay (Promega, Mannheim, Germany), and apoptosis by Caspase-Glo 3/7 Assay. For the assessment of osteoblastic differentiation, we used alizarin red S staining.

RNA isolation, RT, and real-time PCR

RNA from cell cultures was isolated using the HighPure RNA extraction kit from Roche according to the manufacturer's protocol. Five-hundred nanogram RNA was reverse-transcribed using Superscript II (Invitrogen) and subsequently used for SYBR green-based real-time PCR reactions using a standard protocol (Roche). The results were calculated applying the ΔΔCT method and are presented in *x*-fold increase relative to β-actin.

Real-time deformability cytometry

MSC from healthy donors and patients with MDS were treated with 0.1 μM rigosertib for 7 days. After trypsinization, cells in suspension were centrifuged at 115×*g* for 5 min (5805 R, Eppendorf) and resuspended in a solution of PBS without Mg^{2+} and Ca^{2+} (PBS−) and 0.5% (*w*/*v*) methylcellulose (Sigma-Aldrich) to a final concentration of 10^6 cells/ml. Cells have been driven through a microfluidic chip made of poly(dimethylsiloxane) (PDMS; Sylgard 184, VWR) containing two reservoirs connected by a 300-μm long channel with a cross section of 30 × 30 μm. Cell were driven through the constriction at a constant flow rate of 0.32 μL s^{-1}. In real-time cell, cross-sectional area (size) and deformation were estimated and plotted against each other. Statistical analyses were carried out using one-dimensional linear mixed model that incorporates fixed effect parameters and random effects to analyze differences between cell subsets and replicate variances, respectively. *p* values were determined by a likelihood ratio test, comparing the full model with a model lacking the fixed effect term. As a reference, size and deformation of the non-deformed cells in the reservoir were confirmed for all experiments [19].

Co-culture experiments

Primary human MSC were plated at a density of 1–2 × 10^4/cm^2 in DMEM with 10% FCS and pre-treated with rigosertib 0.1 μM or 1.0 μM for 7 days. A 4-week cobblestone area–forming cell (CAFC) assay was performed with or without pre-treatment of the MSC layer. Therefore, 1 × 10^3 magnetically isolated $CD34^+$ cells were co-cultured using LTC-IC media (Stem Cell Technologies, Cologne, Germany) supplemented with 1 × 10^{-6} M hydrocortisone (Sigma-Aldrich, Munich, Germany). After 4 weeks, cells were harvested and 1 × 10^4 cells were plated in enriched methylcellulose medium

with recombinant cytokines (MethoCult H4435, Stem Cell Technology) to perform a colony-forming unit (CFU) assay. After 2 weeks, colonies were counted and classified under a microscope.

Statistical analysis

Results are presented as means ± standard deviation (SD). All experiments were repeated at least three times. Statistical evaluations of two group comparisons were performed using a two-sided Student test. One-way analysis of variance (ANOVA) was used for experiments with more than two groups or time/dose experiments. p values < 0.05 were considered statistically significant.

Results

Effects of rigosertib in young healthy C57BL/6J mice

To investigate the effect of rigosertib on bone and blood parameters in vivo, 10-week-old healthy C57BL/6J wild-type (WT) mice were treated with vehicle or rigosertib (250 mg/kg, 3×/week, i.p.) for 3 weeks. Two days after the last administration, the blood count was measured. Rigosertib treatment induced pancytopenia (Fig. 1), whereas the number of neutrophils, monocytes, and lymphocytes was not affected (data not shown). As a result, we investigated whether this was a direct effect of rigosertib on HSPCs. Bone marrow cells were harvested from the femur of rigosertib-treated mice and analyzed by flow cytometry regarding the number of early- and late-stage erythropoiesis as well as LSK hematopoietic stem cells by flow cytometry. Differences between control and treatment groups were not detectable (Online Resource, Fig. 1). Although we could not exclude functional changes, indirect effects on the cellular compartment of the niche (i.e., stromal cells) may be responsible for the observed blood changes.

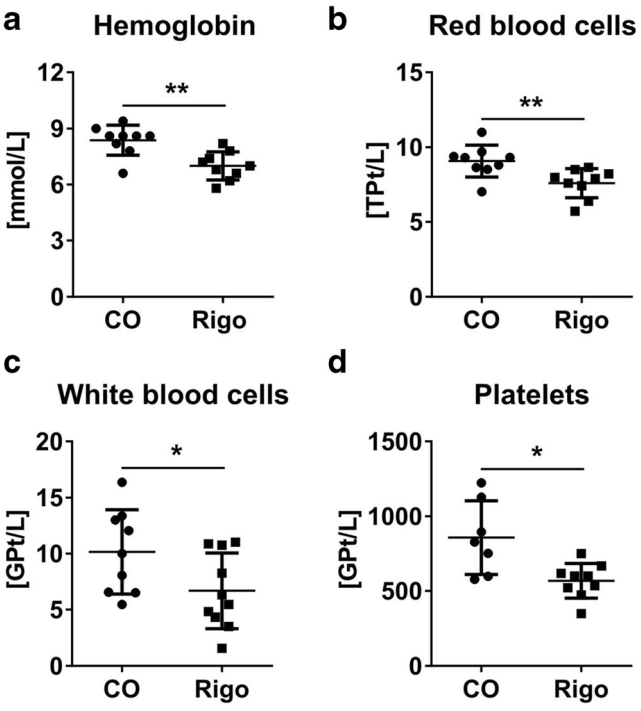

Fig. 1 Blood parameter (**a** hemoglobin; **b** red blood cells; **c** white blood cells; **d** platelets) of wild-type mice upon treatment with vehicle (control, CO) or rigosertib (Rigo) 250 mg/kg for 3 weeks, revealing pancytopenia following rigosertib treatment; *$p < 0.05$, **$p < 0.01$; $n = 7$–10

To further assess the bone homeostasis, micro-computed tomography (μCT) was used to analyze the trabecular bone of the femora and vertebrae of the treated mice. Neither bone volume nor bone microarchitecture (trabecular number, thickness, and separation) in the femur was affected by rigosertib (Online Resource, Fig. 2). However, it reduced trabecular bone volume in the spine (− 16%, $p = 0.05$), which was accompanied by a lower trabecular number and thickness (− 6% and − 10%, respectively, $p < 0.05$; Fig. 2a–c). Rigosertib increased the number of osteoclasts and the osteoclast-covered bone surface, as measured by histomorphology (Fig. 2d, e). In addition, procollagen type 1 N-terminal peptide (P1NP), a serum marker of bone formation, and the bone resorption marker C-terminal collagen type I (CTX-I) were measured. Both parameters were unaffected by rigosertib treatment (Online Resource, Fig. 3). Additionally, we assessed the Wnt pathway, which is one of the most important regulators of bone homeostasis, and measured the level of Wnt inhibitors sclerostin and dickkopf 1 (Dkk-1). However, rigosertib treatment did not alter the serum level of both markers (Online Resource, Fig. 3).

To clarify the functional changes at the cellular level after rigosertib treatment, we isolated MSC from mice treated with rigosertib or vehicle and found no difference in viability immediately after isolation, whereas after 5 days in culture, MSC from rigosertib-treated mice demonstrated significantly reduced viability (− 27%, $p < 0.01$; Fig. 2f). However, this was not due to changes in the rate of apoptosis, as it did not differ in the treated group vs. control group both on day 0 and day 5 of culture (Online Resource, Fig. 4). Similarly, there were no differences in osteogenic differentiation of MSC isolated from mice treated with rigosertib, as analyzed by a mineralization assay and ALP activity (Online Resource, Fig. 5).

Experiments in MDS mouse model NUP98-HOXD13

To study the effects of rigosertib treatment in vivo specifically in MDS, the well-established NUP98-HOXD13 (NHD13) MDS model was used. At the age of 4–6 months, NHD13 mice intrinsically develop MDS-like symptoms including cytopenia as well as dysplastic blood and bone marrow cells. To analyze the effect of rigosertib on the osteo-hematopoietic niche, 5-month-old NHD13 mice and littermate WT control

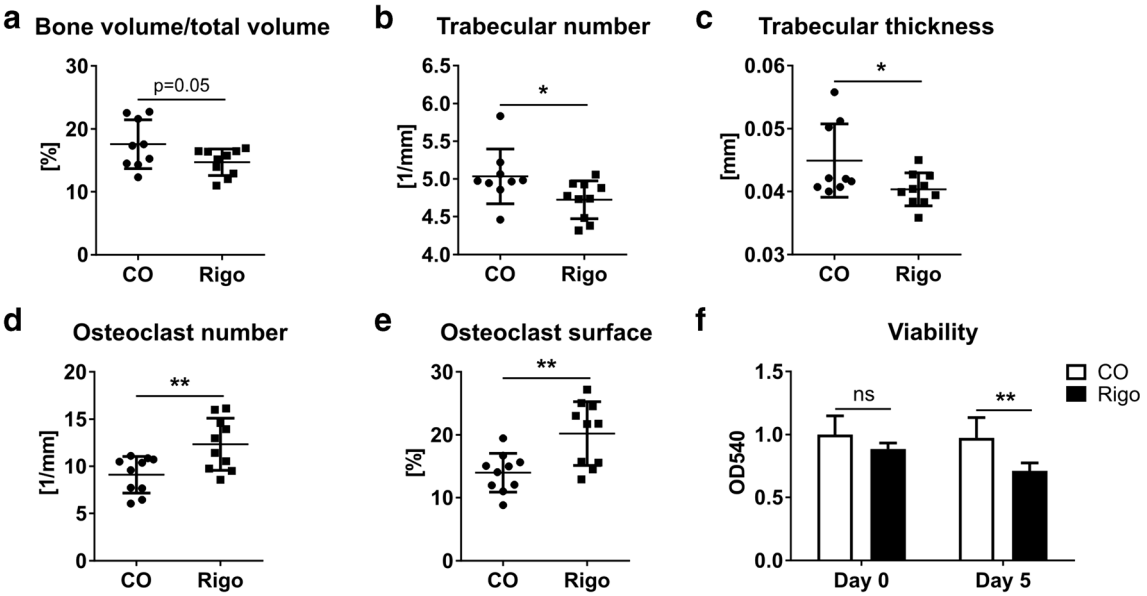

Fig. 2 Bone parameter assessed by µCT in vehicle or rigosertib-treated WT mice, showing a trend towards reduced trabecular bone mass in vertebral bodies (**a**), as well as reduced trabecular number (**b**) and thickness (**c**) upon treatment. Increase in osteoclast number (**d**) and osteoclast surface (**e**) following treatment with rigosertib, assessed by histology. $*p < 0.05$, $**p < 0.01$, for each group $n = 9–10$. **f** Cell viability of MSC isolated from WT mice treated with rigosertib (Rigo) or vehicle (control, CO) demonstrating reduced viability after 5 days of culturing ex vivo (without rigosertib). $**p < 0.01$; ns, not significant; for each group $n > 3$

mice were treated with vehicle or rigosertib (250 mg/kg, 3×/week, i.p.) for 3 weeks. Before treatment, NHD13 mice exhibited decreased hemoglobin levels (− 19%, $p < 0.001$), a reduced number of red blood cells (− 25%, $p < 0.001$), leukocytes (− 78%, $p < 0.001$), and platelets (− 40%, $p < 0.001$) compared with WT mice, which was in line with previous publications [20]. As opposed to younger healthy mice, rigosertib treatment had no effect on red and white blood cells in both groups (Online Resource, Fig. 6), but platelet count was increased in WT mice (+ 26%, $p < 0.05$; Online Resource, Fig. 6). In addition, we could not detect any difference in LSK hematopoietic stem cell and early as well as late erythroblast populations in the bone marrow upon treatment with rigosertib in NHD13 mice or age-matched healthy controls, but it reduced the percentage of reticulocytes in NHD13 mice (− 58%, $p < 0.05$; Online Resource, Fig. 7).

After 3 weeks of rigosertib treatment, bones were collected for µCT analysis. As expected and previously published [21],

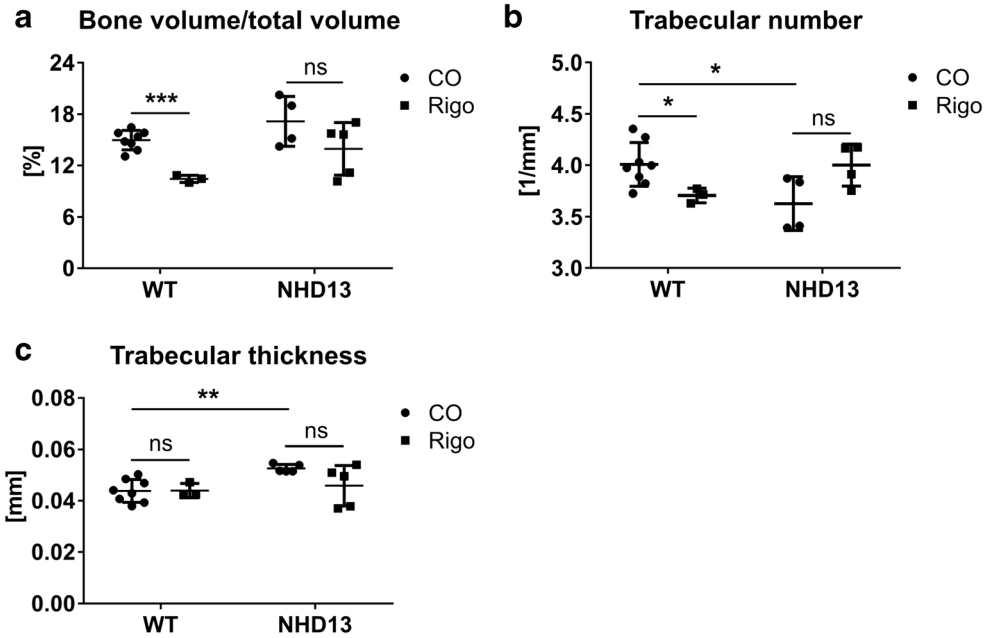

Fig. 3 Bone parameter (**a**, bone volume/total volume (BV/TV); **b**, trabecular number; **c**, trabecular thickness) assessed by µCT in vertebral bodies of 24-week-old NHD13 and WT control mice treated with vehicle or rigosertib. $*p < 0.05$; ns, not significant; $n = 3–8$

NHD13 control mice had an unaltered femoral bone volume but the microarchitecture was changed compared with WT control mice. Rigosertib did not further affect the bone volume, trabecular number, thickness, or separation at the femur of WT or NHD13 mice (Online Resource, Fig. 8). As opposed to WT mice (− 30%, $p < 0.001$), in NHD13 mice, rigosertib treatment only slightly reduced trabecular bone volume in vertebrae (Fig. 3a). Interestingly, whereas initial trabecular number in vertebral bodies was significantly lower in NHD13 mice compared with control mice (− 11%, $p < 0.05$), rigosertib treatment increased trabecular number in transgenic mice, so that we could not detect any difference to untreated WT mice (Fig. 3b). Trabecular thickness in vertebral bodies, which is significantly higher in NHD13 mice (+ 21%, $p < 0.01$; Fig. 3c), was not affected by treatment with rigosertib in both, WT and transgenic NHD13 mice.

In vitro experiments with human young healthy, old healthy, and MDS-MSC

To validate the results obtained in mice, we performed further experiments in vitro, using material from patients with MDS and healthy controls. First, we assessed the effect of different concentrations of rigosertib on cell viability in MSC from young healthy donors. After 7 days of treatment, the viability was significantly reduced starting from a concentration of 0.5 μM (Fig. 4a). Lower concentrations of rigosertib as 0.1 μM and 0.05 μM did not affect cell viability. Therefore, we chose a concentration of 0.1 μM for further experiments with MDS-MSC and MSC from age-matched healthy controls. Rigosertib did not affect cell viability and apoptosis rate in MDS-MSC and age-matched healthy MSC (Fig. 4b, c). Differences in the mRNA expression of genes affecting the cell cycle (p21, p53, p27, BCL2, survivin, CCND1) were also not detected (data not shown). Osteoblastic differentiation potential of MSC derived from MDS patients and old healthy donors was not affected by rigosertib (Fig. 4d). In parallel, no difference in expression of ALP was detected in rigosertib-treated MDS-MSC (1.12-fold, $p = 0.63$).

As one of rigosertib's mechanisms of action is destabilizing microtubules [5], we assumed that biomechanical characteristics of the rigosertib-treated cells would be affected, and thus tested the mechanical properties of treated MSC. When we used the novel label-free method for the biomechanical characterization of cells—real-time deformability cytometry—we observed that in certain cases, the initially morphologically homogenous

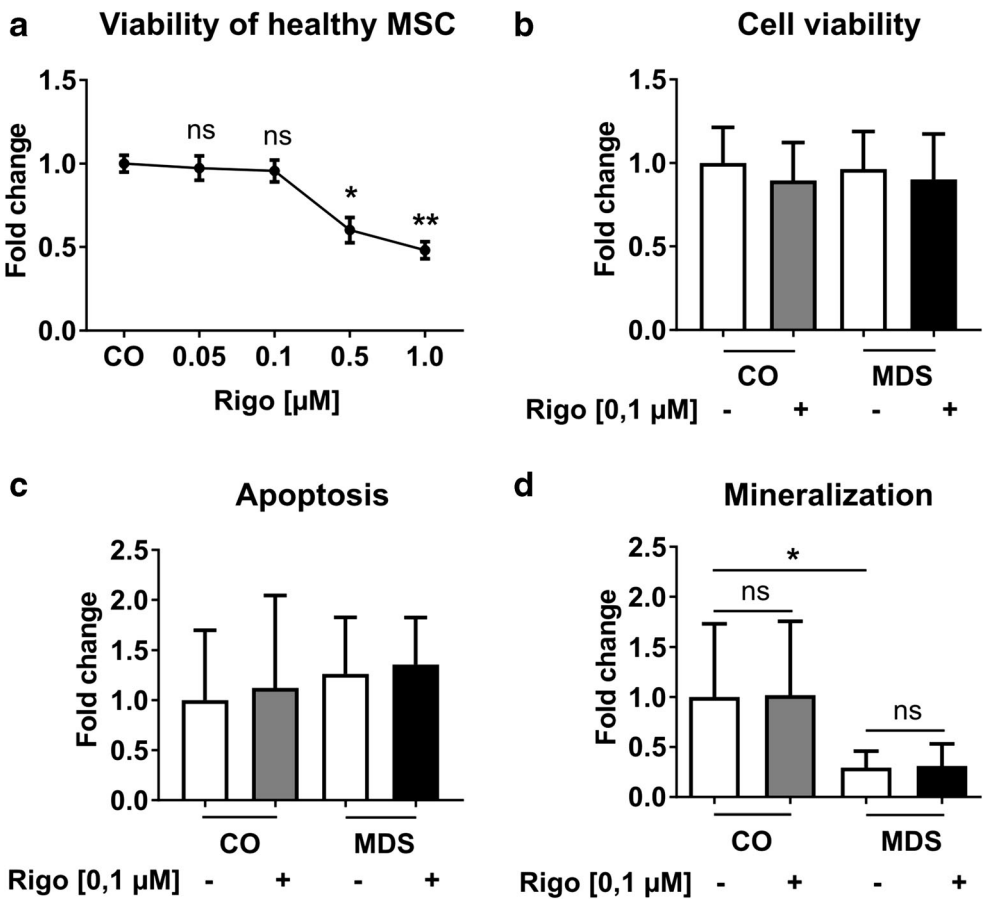

Fig. 4 **a** After 7 days of treatment, viability of healthy MSC from young donors is dependent on the concentration of rigosertib and is significantly reduced at the concentration ≥ 0.5 μM. **b** Cell viability and apoptosis (**c**) of healthy old MSC (CO) and MDS-MSC were not significantly affected after 7 days of treatment with 0.1 μM rigosertib. **d** Osteoblastic differentiation, as measured by alizarin staining, demonstrating no significant influence on differentiation capacity of old healthy (CO) and MDS-MSC after treatment with 0.1 μM rigosertib.*$p < 0.05$; ns, not significant; for each group $n > 3$

MSC population was divided into two distinct groups with a minor fraction of smaller and stiffer cells and a larger population of softer cells (representative example is demonstrated in Fig. 5a), suggesting different sensitivities of MSC subgroups from the same donor towards rigosertib. Generally, elastic modulus of rigosertib-treated young healthy MSC was significantly higher than prior to treatment, meaning that the healthy cells became on the average stiffer after the treatment, whereas only three out of five MDS-MSC demonstrated such effect (Fig. 5b, c).

To clarify signaling pathways which are involved in the observed rigosertib effects on the MSC, we analyzed the phosphorylation status of several signaling molecules, which have been previously described to be influenced by rigosertib (mTOR, AKT, p42/44, IκB) by Western blot and found no activation or downregulation of these pathways in MDS-MSC (data not shown).

Finally, we investigated how rigosertib affects the support of hematopoiesis by MSC. Therefore, we investigated the colony-forming potential of pre-treated MSC in long-term co-cultures with CD34+ HSPC. The number of cobblestone area–forming cells (CAFC) as readout for an active stromal support was significantly reduced in rigosertib-pretreated MSC from both healthy donors and MDS patients at different rigosertib concentrations (Fig. 6a). To study the clonogenic potential of HSPCs cultured on pretreated MSC layers, a colony-forming unit (CFU) assay was performed. Compared with controls, the total number of colonies was significantly reduced in co-cultures with rigosertib-pretreated MSC from MDS patients, but not from healthy donors (Fig. 6b, c). Most markedly, the differentiation of the monocytic lineage was affected (Fig. 6c).

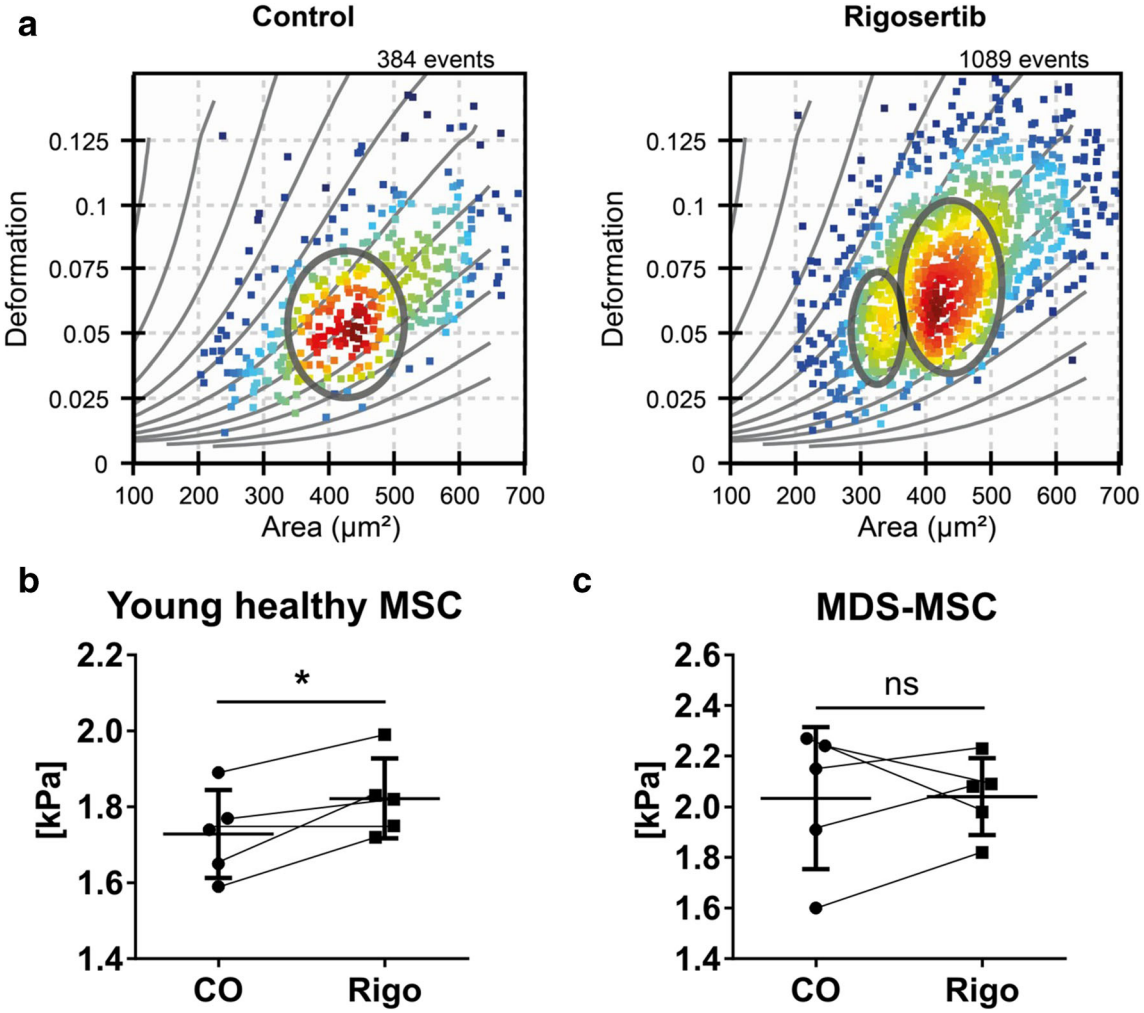

Fig. 5 Biomechanical properties of MSC from young healthy donors and MDS patients measured by real-time deformability cytometry (RT-DC). A representative RT-DC plot (**a**) demonstrates the formation of two biomechanical populations after rigosertib treatment. **b** Young healthy MSC became significantly stiffer after treatment with rigosertib, evaluated by the higher elastic Young's modulus, whereas the elastic modulus of MDS-MSC remains unchanged (**c**). *$p < 0.05$; ns, not significant; $n = 5$ for each group

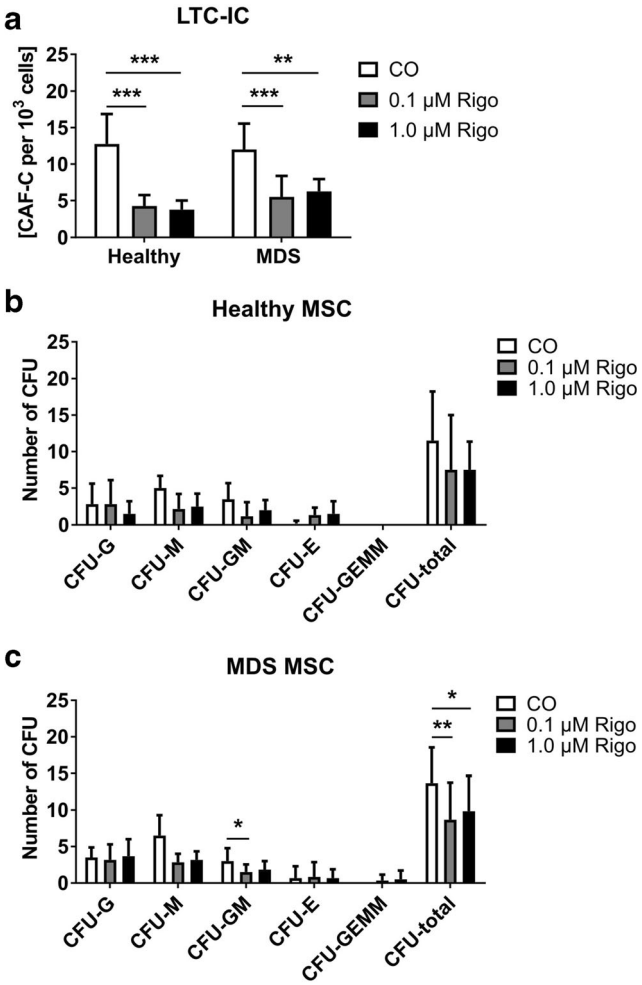

Fig. 6 Human mesenchymal stromal cells were pretreated with rigosertib 0.1 μM or 1.0 μM for 7 days and co-cultured with freshly isolated CD34+ HSPC. **a** After 4 weeks of co-culture, the number of CAF-C was determined in each well. A CFU assay was performed in methylcellulose medium for additional 2 weeks and the colonies were classified under a microscope for HSPC co-cultured with **b** healthy MSC and **c** MDS-MSC. $n = 3–5$. $^{*}p < 0.05$, $^{**}p < 0.01$, $^{***}p < 0.001$

Discussion

Rigosertib (ON 01910.Na) is an investigational drug, which is being clinically developed for the therapeutic management of high-risk MDS failing HMA-based therapy. Here, we present a comprehensive assessment of the effects of rigosertib on the cellular components of the osteo-hematopoietic microenvironment. First of all, we performed in vivo experiments using young healthy mice and observed that treatment with rigosertib resulted in cytopenia. According to previous publication, a direct effect on HSPCs is rather unlikely [9]. In line with that, we could not detect any difference in the frequency of LSK cells. Although the effect of rigosertib on bone parameters was moderate with only mildly reduced trabecular bone mass accompanied by lower trabecular thickness and number in vertebral bodies, it might be sufficient to disturb the intercellular connections at the molecular level. In order to verify this hypothesis, we isolated MSC from treated mice and detected a reduced viability after 5 days of culturing compared with the cells from untreated mice.

Moreover, we have tested the effects of rigosertib on bone marrow niche cells in myelodysplastic mice. We assessed bone and blood parameters in 24-week-old NHD13 transgenic mice after 3 weeks of treatment with rigosertib. Therein, we could confirm previous observations published by our group [21], demonstrating normal trabecular bone volume, decreased trabecular number, and increased trabecular separation as well as trabecular thickness in NHD13 mice compared with age-matched littermates. Over all, rigosertib did not greatly affect bone homeostasis. It only showed effects in the axial skeleton, but not in the long bones, which is possibly explainable through the prevalent trabecular structure in the axial skeleton which therefore displays a larger surface area for effects on bone remodeling. Moreover, rigosertib did not affect any blood parameters (as opposed to young healthy mice) as well as LSK population and erythroid precursors, so we speculate that this drug preferentially affects the stromal compartment of the osteo-hematopoietic niche in younger animals, which have a higher bone turnover and likely more active cellular interactions in the osteo-hematopoietic niche. In vitro, only the MSC from young healthy donors became significantly stiffer through rigosertib treatment measured by real-time deformability cytometry (RT-DC), compared with MDS-MSC where only certain patients demonstrated such changes.

In our experiments with MSC from MDS patients, we demonstrate that rigosertib is toxic for MSC in nanomolar concentrations (equal or above 500 nM), although it has been previously postulated that in normal cells, such as lung fibroblasts, rigosertib has little or no effect unless its concentration is greater than 5–10 μM [22]. Interestingly, we observed the different sensitivities of the cells from the same donor towards the rigosertib treatment, as we have seen the formation of two distinct biomechanical populations measured by RT-DC. As the destabilizing of microtubules and disruption of mitosis is one of the known mechanisms of action of this drug [5], possibly only those healthy cells which are actively dividing at the time of treatment are affected and therefore form the second population, which determines the observed mild catabolic effect on MSC/OB. Accordingly, biomechanical properties of MSCs in combination with cell cycle analysis, measured by real-time fluorescence and deformability cytometry (RT-FDC), can possibly underline this results and may allow a more detailed investigation of the distinct biomechanical cell populations and shed light on the biology of the observed effects.

Although the direct effects on stromal cells were relatively mild, it did significantly reduce the hematopoiesis-supporting

capacity of the rigosertib-pretreated MSC, reflecting total number of colony-forming units, as well as monocytic precursors in long-term co-culture experiments. Of note, such suppressing action was only apparent for MDS-MSC, whereas hematopoiesis-supporting capacity of healthy MSC was not deteriorated by the pretreatment with rigosertib. This gives a hint that the components of the osteo-hematopoietic niche in MDS patients in its complex can be more sensitive towards the therapy as in healthy donors.

Taken together, rigosertib acts mostly catabolically with decreased MSC viability (in vitro and ex vivo); increased osteoclast number and surface (in vivo) leading to a decrease in trabecular bone mass, trabecular thickness, and number in young WT mice; decrease in bone mass and trabecular number in elderly WT mice; and slight decrease in bone mass in MDS mouse model. The observed effects on the bone cells appear to indirectly affect hematopoiesis, leading to pancytopenia in young WT mice, which is similar to the most common adverse events observed in the ONTIME trial [10].

In conclusion, rigosertib exerts several inhibitory effects on the cellular components of the osteo-hematopoietic niche. Further investigations could be conducted to clarify if rigosertib acts differently on the osteo-hematopoietic niche from certain MDS patient groups, such as with monosomy 7 or trisomy 8, as these patients tend to respond to rigosertib better than other MDS subgroups.

Acknowledgments The authors would like to thank Eva Schubert, Tina Dybek, Marie-Christin Mehnert, Anja Liebkopf, and Ivonne Habermann for technical assistance as well as Dr. Maik Stiehler for the provided material from the elderly healthy donors.

Funding Funding for this study was provided in part by the Shire Deutschland GmbH.

Compliance with ethical standards

Ethical approval All procedures performed in studies involving human participants were in accordance with the ethical standards of the institutional research committee and with the 1964 Helsinki Declaration and its later amendments or comparable ethical standards. Informed consent was obtained from all individual participants included in the study.

All animal procedures were approved by the institutional animal care committee and the Federal state of Saxony. All applicable international, national, and institutional guidelines for the care and use of animals were followed.

Conflict of interest The authors have received grants or honorarium for advisory boards or lectures to the individual or the institution from Novartis (UP, MB, LCH), Celgene (MB, UP), Amgen (LCH, MR), Alexion (LCH), and Shire (LCH). UP and LCH are supported by a grant within the German Consortium of translational cancer research (DKTK), UP/MB/LCH are supported by the Sonderforschungsbereich (SFB) 655 from the Deutsche Forschungsgemeinschaft (DFG), UP/MR are supported by a grant from the Deutsche José Carreras Leukämie-Stiftung, and LCH is supported by a seed grant from the CRTD. Financial support from Alexander von Humboldt Stiftung (Alexander von Humboldt professorship to JG), Sächsisches Ministerium für Wissenschaft und Kunst (TG70 grant to JG), an ERC Starting Grant (starting grant "LightTouch" #282060 to JG), and DKMS "Mechthild Harf Research Grant" (DKMS-SLS-MHG-2016-02 to AJ) are gratefully acknowledged. All other authors report no conflicts of interest.

References

1. Athuluri-Divakar SK, Vasquez-Del Carpio R, Dutta K et al (2016) A small molecule RAS-mimetic disrupts RAS association with effector proteins to block signaling. Cell 165:643–655. https://doi.org/10.1016/j.cell.2016.03.045
2. Ritt DA, Abreu-Blanco MT, Bindu L, Durrant DE, Zhou M, Specht SI, Stephen AG, Holderfield M, Morrison DK (2016) Inhibition of Ras/Raf/MEK/ERK pathway signaling by a stress-induced phospho-regulatory circuit. Mol Cell 64:875–887. https://doi.org/10.1016/j.molcel.2016.10.029
3. Prasad A, Park IW, Allen H, Zhang X, Reddy MVR, Boominathan R, Reddy EP, Groopman JE (2009) Styryl sulfonyl compounds inhibit translation of cyclin D1 in mantle cell lymphoma cells. Oncogene 28:1518–1528. https://doi.org/10.1038/onc.2008.502
4. Prasad A, Khudaynazar N, Tantravahi RV et al (2016) ON 01910.Na (rigosertib) inhibits PI3K/Akt pathway and activates oxidative stress signals in head and neck cancer cell lines. Oncotarget 7:79388–79400. https://doi.org/10.18632/oncotarget.12692
5. Jost M, Chen Y, Gilbert LA et al (2017) Combined CRISPRi/a-based chemical genetic screens reveal that rigosertib is a microtubule-destabilizing agent. Mol Cell 68:210–223.e6. https://doi.org/10.1016/j.molcel.2017.09.012
6. Hyoda T, Tsujioka T, Nakahara T, Suemori SI, Okamoto S, Kataoka M, Tohyama K (2015) Rigosertib induces cell death of a myelodysplastic syndrome-derived cell line by DNA damage-induced G2/M arrest. Cancer Sci 106:287–293. https://doi.org/10.1111/cas.12605
7. Dai YH, Hung LY, Chen RY et al (2015) ON 01910.Na inhibits growth of diffuse large B-cell lymphoma by cytoplasmic sequestration of sumoylated C-MYB/TRAF6 complex. Transl Res
8. Sloand EM, Pfannes L, Chen G, Shah S, Solomou EE, Barrett J, Young NS (2007) CD34 cells from patients with trisomy 8 myelodysplastic syndrome (MDS) express early apoptotic markers but avoid programmed cell death by up-regulation of antiapoptotic proteins. Blood 109:2399–2405. https://doi.org/10.1182/blood-2006-01-030643
9. Olnes MJ, Shenoy A, Weinstein B, Pfannes L, Loeliger K, Tucker Z, Tian X, Kwak M, Wilhelm F, Yong ASM, Maric I, Maniar M, Scheinberg P, Groopman J, Young NS, Sloand EM (2012) Directed therapy for patients with myelodysplastic syndromes (MDS) by suppression of cyclin D1 with ON 01910.Na. Leuk Res 36:982–989. https://doi.org/10.1016/j.leukres.2012.04.002
10. Garcia-Manero G, Fenaux P, Al-Kali A et al (2016) Rigosertib versus best supportive care for patients with high-risk myelodysplastic syndromes after failure of hypomethylating drugs (ONTIME): a randomised, controlled, phase 3 trial. Lancet Oncol 17:496–508. https://doi.org/10.1016/S1470-2045(16)00009-7
11. Silverman LR, Greenberg P, Raza A, Olnes MJ, Holland JF, Reddy P, Maniar M, Wilhelm F (2015) Clinical activity and safety of the dual pathway inhibitor rigosertib for higher risk myelodysplastic syndromes following DNA methyltransferase inhibitor therapy. Hematol Oncol 33:57–66. https://doi.org/10.1002/hon.2137
12. Seetharam M, Fan AC, Tran M, Xu L, Renschler JP, Felsher DW, Sridhar K, Wilhelm F, Greenberg PL (2012) Treatment of higher risk myelodysplastic syndrome patients unresponsive to hypomethylating agents with ON 01910.Na. Leuk Res 36:98–103. https://doi.org/10.1016/j.leukres.2011.08.022

13. Komrokji RS, Raza A, Lancet JE, Ren C, Taft D, Maniar M, Wilhelm F, List AF (2013) Phase I clinical trial of oral rigosertib in patients with myelodysplastic syndromes. Br J Haematol 162: 517–524. https://doi.org/10.1111/bjh.12436
14. Navada SC, Fruchtman SM, Odchimar-Reissig R, Demakos EP, Petrone ME, Zbyszewski PS, Holland JF, Silverman LR (2018) A phase 1/2 study of rigosertib in patients with myelodysplastic syndromes (MDS) and MDS progressed to acute myeloid leukemia. Leuk Res 64:10–16. https://doi.org/10.1016/j.leukres.2017.11.006
15. Chapman CM, Sun X, Roschewski M, Aue G, Farooqui M, Stennett L, Gibellini F, Arthur D, Perez-Galan P, Wiestner A (2012) ON 01910.Na is selectively cytotoxic for chronic lymphocytic leukemia cells through a dual mechanism of action involving PI3K/AKT inhibition and induction of oxidative stress. Clin Cancer Res 18:1979–1991. https://doi.org/10.1158/1078-0432.CCR-11-2113
16. Bulycheva E, Rauner M, Medyouf H, Theurl I, Bornhäuser M, Hofbauer LC, Platzbecker U (2015) Myelodysplasia is in the niche: novel concepts and emerging therapies. Leukemia. 29:259–268. https://doi.org/10.1038/leu.2014.325
17. Balaian E, Wobus M, Weidner H, Baschant U, Stiehler M, Ehninger G, Bornhäuser M, Hofbauer LC, Rauner M, Platzbecker U (2018) Erythropoietin inhibits osteoblast function in myelodysplastic syndromes via the canonical Wnt pathway. Haematologica. 103:61–68. https://doi.org/10.3324/haematol.2017.172726
18. Rauner M, Stein N, Winzer M, Goettsch C, Zwerina J, Schett G, Distler JHW, Albers J, Schulze J, Schinke T, Bornhäuser M, Platzbecker U, Hofbauer LC (2012) WNT5A is induced by inflammatory mediators in bone marrow stromal cells and regulates cytokine and chemokine production. J Bone Miner Res 27:575–585. https://doi.org/10.1002/jbmr.1488
19. Otto O, Rosendahl P, Mietke A, Golfier S, Herold C, Klaue D, Girardo S, Pagliara S, Ekpenyong A, Jacobi A, Wobus M, Töpfner N, Keyser UF, Mansfeld J, Fischer-Friedrich E, Guck J (2015) Real-time deformability cytometry: on-the-fly cell mechanical phenotyping. Nat Methods 12:199–202. https://doi.org/10.1038/nmeth.3281
20. Lin YW, Slape C, Zhang Z, Aplan PD (2005) NUP98-HOXD13 transgenic mice develop a highly penetrant, severe myelodysplastic syndrome that progresses to acute leukemia. Blood 106:287–295. https://doi.org/10.1182/blood-2004-12-4794
21. Weidner H, Rauner M, Trautmann F, Schmitt J, Balaian E, Mies A, Helas S, Baschant U, Khandanpour C, Bornhäuser M, Hofbauer LC, Platzbecker U (2017) Myelodysplastic syndromes and bone loss in mice and men. Leukemia 31:1003–1007
22. Gumireddy K, Reddy MVR, Cosenza SC, Nathan RB, Baker SJ, Papathi N, Jiang J, Holland J, Reddy EP (2005) ON01910, a non-ATP-competitive small molecule inhibitor of Plk1, is a potent anticancer agent. Cancer Cell 7:275–286. https://doi.org/10.1016/j.ccr.2005.02.009